Biochem. J. (1989) 264, 265–273 (Printed in Great Britain)

Electrochemical and spectroscopic characterization of the 7Fe form of ferredoxin III from *Desulfovibrio africanus*

Fraser A. ARMSTRONG,* Simon J. GEORGE,† Richard CAMMACK,‡ E. Claude HATCHIKIAN§ and Andrew J. THOMSON†‖

* Inorganic Chemistry Laboratory, University of Oxford, South Parks Road, Oxford OX1 3QR, U.K., † School of Chemical Sciences, University of East Anglia, Norwich NR4 7TJ, U.K., ‡ Department of Biochemistry, King's College, London WC2R 2LS, U.K., and § Laboratoire de Chimie Bacterienne, C.N.R.S., P.B. 71, 13277 Marseille, France

Desulfovibrio africanus ferredoxin III is a monomeric protein (M_r 6585) containing seven cysteine residues and 7–8 iron atoms and 6–8 atoms of acid-labile sulphur. It is shown that reversible unmediated electrochemistry of the two iron–sulphur clusters can be obtained by using a pyrolytic-graphite-'edge' carbon electrode in the presence of an appropriate aminoglycoside, neomycin or tobramycin, as promoter. Cyclic voltammetry reveals two well-defined reversible waves with $E^{0'} = -140 \pm 10$ mV and -410 ± 5 mV (standard hydrogen electrode) at 2 °C. Bulk reduction confirms that each of these corresponds to a one-electron process. Low-temperature e.p.r. and magnetic-c.d. spectroscopy identify the higher-potential redox couple with a cluster of core $[3Fe\text{-}4S]^{1+,0}$ and the lower with a $[4Fe\text{-}4S]^{2+,1+}$ centre. The low-temperature magnetic-c.d. spectra and magnetization properties of the three-iron cluster show that it is essentially identical with that in *Desulfovibrio gigas* ferredoxin II. We assign cysteine-11, -17 and -51 as ligands of the [3Fe-4S] core and cysteine-21, -41, -44 and -47 to the [4Fe-4S] centre.

INTRODUCTION

The recent redeterminations [1,2] of the tertiary structure of *Azotobacter vinelandii* ferredoxin (Fd) I reveal two clusters, one comprising a [4Fe-4S] core co-ordinated by four cysteine residues (numbers 20, 39, 42 and 45) and the other having a [3Fe-4S] core liganded by only three cysteine residues (numbers 8, 16 and 49). The fold of the polypeptide chain is similar to that of the homologous 8Fe Fd from *Peptococcus aerogenes* [3] for the *N*-terminal half of the sequence. The *C*-terminal residues wrap around this structure. Two cysteine residues, numbers 11 and 24, are left un-co-ordinated to either metal centre. Thus in principle a ferredoxin containing only seven cysteine residues suitably placed in its primary sequence should be able to co-ordinate one [4Fe-4S] and one [3Fe-4S] core cluster. Fd III from *Desulfovibrio africanus* strain Benghazi (N.C.I.B. 8401) has seven cysteine residues only per monomer of protein and has a known amino acid sequence [4]. In the present paper we show, by a combination of novel electrochemical analysis [using direct electrochemistry of the protein at a pyrolytic-graphite-edge (PGE) electrode] and characterization of species by e.p.r. and m.c.d. spectroscopy, that Fd III (*D. africanus*) is a 7Fe protein containing two clusters, one [4Fe-4S] and one [3Fe-4S]. In the following paper [5] we show further that, in spite of the presence of only 7 cysteine residues, the 7Fe form of Fd III rapidly takes up one further iron to yield an 8Fe ferredoxin of unique magnetic properties.

Three distinct ferredoxins have been isolated from *D. africanus* [4,6,7]. We have previously shown that Fd I contains a $[4Fe\text{-}4S]^{2+,1+}$ cluster within a polypeptide with an M_r of 6700 and that Fd II contains a spectroscopically similar 4Fe centre within a slightly smaller polypeptide [8]. As isolated, the Fd III polypeptide has a monomeric M_r of 6585 and contains 7–8 atoms of Fe and 6–8 atoms of acid-labile sulphide ion per monomer [4]. Previously Fd III has been reported to be a dimer [6]; however, recent equilibrium-sedimentation results indicate that this protein is a monomer (E. C. Hatchikian, unpublished work). The amino acid sequence shows it to be similar in structure to *Clostridium* and *Desulfovibrio* ferredoxins [4]. Two parts of the sequence, namely Cys^{21}-Pro and Cys^{41}-Leu-Gly-Cys^{44}-Glu-Ser-Cys^{47}, provide a typical binding domain for one [4Fe-4S] cluster. A second iron-binding domain comprises Cys^{51}-Glu and Cys^{11}-Thr-Gly-Asp-Gly-Glu-Cys^{17}. The remote cysteine residue (position 51) is next to a glutamic acid residue rather than the usual common proline group. More interesting still, position 14, which would normally be cysteine, is aspartic acid. Aspartate is not known to be a ligand to iron–sulphur clusters, but it is possible that this type of ligation will occur. Therefore, this second metal-binding domain provides a potential donor set of three cysteine ligands (numbers 11, 17 and 51) and one aspartic acid residue (number 14) that may bind a 3Fe centre or provide a novel co-ordination site for a [4Fe-4S] cluster. The evidence presented in this and the following paper [5] leads us to propose that both situations can arise in *D. africanus* Fd III. This ferredoxin therefore represents an interesting template of ligands for defining cluster type, for examining cluster transformation and for studying the effects of non-cysteinyl ligation on iron–sulphur clusters.

We demonstrate in this paper that rapid and reversible

Abbreviations used: Fd, ferredoxin; m.c.d., magnetic circular dichroism; HDTA, hexenediaminetetra-acetic acid; PGE, pyrolytic graphite edge.

‖ To whom correspondence should be addressed.

electron transfer can be established between a PGE electrode and both of the iron–sulphur clusters of the protein in the presence of an appropriate aminoglycoside, neomycin or tobramycin, as a promoter of interfacial interaction. This enables cyclic voltammetric analysis of the clusters to be carried out and cluster transformation to be readily observed and monitored. Low-temperature e.p.r. and m.c.d. spectroscopies have been used to identify and quantify cluster types.

METHODS

Protein preparation

Fd III was isolated from *D. africanus* strain Benghazi (N.C.I.B. 8401) by using the procedure previously described [6], and stored as frozen pellets in liquid N_2. The final protein gave a single band upon SDS/polyacrylamide-gel electrophoresis and had a purity index (A_{408}/A_{280}) of 0.78. Concentrations were determined by using the absorption coefficient 28.6 $mM^{-1} \cdot cm^{-1}$.

For most of this work, thawed pellets were dialysed at 4 °C against buffer solutions in an Amicon diafiltration unit equipped with a YM5 membrane and a microvolume assembly. For the direct (unmediated) electrochemical studies, final solutions were typically 60–120 μM-Fd III in 20 mM-Hepes buffer, pH 7.3–7.5, containing 100 mM-NaCl or -$NaClO_4$. Two approaches were made for the study of pH effects on potentials. In one, Pipes or Taps buffers were simply substituted for Hepes to give solutions at pH 6.3 and 8.4 respectively. Alternatively, the protein was dialysed into a mixed-buffer electrolyte (3 mM each in Pipes, Hepes and Taps with 100 mM-NaCl) and the pH was varied *in situ* by addition of small portions of HCl or NaOH. For certain spectroscopy experiments more concentrated protein (approx. 400 μM) was required. For the low-temperature m.c.d. measurements, protein, usually in 40 mM-Hepes buffer containing 200 mM-NaCl, was diluted to 50% (v/v) with ethanediol, thereby enabling the formation of an optical-quality glass on freezing. Control e.p.r. and c.d. experiments were performed to ensure that the protein was unaffected by the glycol glassing agent. All reagents used were of the highest available commercial quality.

Reductions were usually performed electrochemically in the apparatus described below. Chemical reductions were achieved by addition of microlitre quantities of 100 mM-$Na_2S_2O_4$ solution to degassed protein at 4 °C in an anaerobic glovebox ($O_2 < 1$ p.p.m.). Care was taken to add only a minimal excess of this reductant. Chemical preparation of partially reduced protein samples was carried out with phenosafranine as a redox buffer. This organic dye was chosen not only because of its appropriate redox potential ($E^{0'} = -252$ mV) but because this was relatively insensitive to the addition of ethanediol.

It was found very early on in our investigation that it was important to quench the activity of extraneous iron. Unless stated otherwise, all apparatus with which protein came into contact was soaked in EDTA or EGTA solutions and rinsed thoroughly with distilled or deionized water. Buffers also normally contained 0.1 mM- or 2 mM-EDTA, -HDTA or -EGTA. The last of these was found to be the most suitable iron chelator for the direct electrochemical experiments because the higher redox potential [$E^{0'}$ versus standard hydrogen electrode at pH 7.3: Fe(EGTA) = +250 mV, Fe(EDTA) = +105 mV, Fe(HDTA) did not give clean electrochemistry] allowed voltammetric sweeps to potentials as high as +230 mV without interference or distortion of background. Traces of extraneous iron could always be detected by cycling up to +400 mV and down again.

Direct (unmediated) electrochemical measurements

Two types of cell configuration were used for direct electrochemistry. For most voltammetric studies an all-glass unit featuring a reference arm and a small-volume sample compartment was employed. The reference arm was equipped with a circulating jacket to maintain the saturated calomel electrode at 25 °C, at which E^0 (standard calomel electrode) = +244 mV versus standard hydrogen electrode. Unless stated otherwise, all potentials quoted in this paper are versus standard hydrogen electrode. The reference was linked to the sample compartment by a long 'salt-bridge' glass tube terminating at a Luggin capillary tip. Typically 600 μl of protein solution was contained in the sample compartment, which was itself immersed in a cooling bath maintained at 2 °C. When required the sample could be stirred magnetically by a 'microflea'. Deoxygenation was achieved by passing humidified Ar across the solution surface while it was stirred. The counter electrode was a piece of platinum gauze positioned opposite to the Luggin tip. The working electrode was a piece of pyrolytic graphite (PG) mounted into a Teflon sheath with the *a–b* plane perpendicular to the solution interface, i.e. 'edge'-oriented (hence PGE). The surface (area 0.18 cm^2) was polished before each set of scans with an aqueous slurry of 0.3 μm-particle-size Al_2O_3 (Banner, Coventry, U.K.) on cottonwool. This was followed by rinsing and sonication to remove traces of Al_2O_3. During voltammetric scans the PGE was positioned close to the Luggin tip. *In situ* pH measurements were made using a micro combination pH electrode (MI-410; Microelectrodes Inc.). Formal redox potentials $E^{0'}$ were determined from the average of oxidative (anodic) and reductive (cathodic) peak potentials, i.e. $(E_{pa} + E_{pc})/2$.

For the combined voltammetric and bulk electrolysis studies a three-chamber glass cell assembly was used inside the anaerobic glovebox. This apparatus is described only briefly in the present paper. The PGE working electrode formed the 'floor' of the jacketed sample compartment, which was thermostatically maintained at 2–3 °C. Efficient stirring of the sample (approx. 400 μl) was achieved by use of a magnetic 'microflea'. Into the solution dipped the ends of reference and auxillary side arms. These were passed through rubber septa in a glass cap, which served to isolate the cell interior from the glovebox atmosphere. The reference side arm comprised a Luggin tip, a long U-shaped salt-bridge tube and a compartment into which was mounted the standard calomel electrode reference through a screw-thread adaptor. The auxillary side arm featured a Vycor conducting glass plug at the end that was in contact with the sample solutions. This was attached via heatshrink tubing to a U-shaped connecting tube leading to a compartment into which was placed a platinum gauze electrode. Typically the central sample cell was cleaned and the electrode was polished with a 1.0 μm-particle-size Al_2O_3/ water slurry on cottonwool 'buds'. This was followed by extensive sonication and repeated several times before transfer into the glovebox. Here it was positioned on a magnetic-stirrer plate and connected to

the coolant circuit. The glass cap and side arms were placed in position, and the sample solution was added by plastic syringe. After electrolysis the sample solution could be withdrawn by syringe and transferred to an e.p.r. tube for freezing.

Interaction of the protein with the electrode surface was promoted by the appropriate aminoglycoside neomycin or tobramycin (Sigma Chemical Co.), which was added as small portions from a 0.2 M stock solution that had been adjusted to pH 7. Final concentrations of aminoglycoside required to optimize the voltammetric response varied, but 1 mM was generally sufficient. No attempt was made in this study to assess the promotion quantitatively. Without neomycin or tobramycin no responses were observed, but weak and unstable waves showing similar potential positions could be obtained by additions of hexamethonium dichloride and even $BaCl_2$ at 0.2 M concentration. Promotion of the direct electrochemistry, at PGE electrodes, of various proteins by multi-charged cations has been described previously [9].

Control of potential and monitoring of current in the direct electrochemistry experiments were carried out with an Oxford electrodes potentiostat.

Mediated electrochemical measurements

Determinations of reduction potentials were also made by using the more usual technique of adjustment of the potential of the protein in the presence of mediator dyes, followed by measurement of the e.p.r. signals. Measurements at higher potentials (200 to −200 mV) were made with the mediators (all at 40 μM concentrations) hydroquinone, Methylene Blue, thionine, Indigodisulphonate, Indigotetrasulphonate and 2-hydroxy-1,4-naphthoquinone, whereas for those at low potentials the mediators (40 μM) were phenosafranine, anthraquinone-2,7-disulphonate, benzyl viologen, methyl viologen, diquat, triquat and *NN'*-dimethyl-3-methyl-4,4'-bipyridylium. The protein solution was reduced and oxidized with small additions of 0.1 M-$Na_2S_2O_4$ and 0.2 M-$K_3Fe(CN)_6$ respectively, stirred in a vessel at 25 °C under Ar. The redox potential was measured by platinum and calomel electrodes. After equilibration at each potential for approx. 2 min a sample was transferred anaerobically with a syringe to an e.p.r. tube and frozen for e.p.r. measurements. The signal amplitudes from samples poised at different potentials were fitted to curves calculated from the Nernst equation, assuming that the clusters are each one-electron carriers.

Spectroscopic measurements

E.p.r. spectra were recorded at Norwich on an X-band Bruker ER-200D spectrometer fitted with a dedicated ASPECT 2000 computer. Temperature control was provided by an Oxford Instruments ESR-900 flow cryostat cooled with liquid He. Spin integrations were performed with a 1 mM-Cu(II)–EDTA solution as a standard. Appropriate corrections were made for differences in the temperature and microwave power used for the sample and the standard. The e.p.r. spectra used to monitor the mediated midpoint reduction potentials were recorded on a Varian E4 spectrometer fitted with an Oxford Instruments ESR 9 liquid-He flow cryostat. Low-temperature m.c.d. measurements were carried out with a JASCO J-500D dichrograph interfaced to a Commodore 710B microcomputer running software written within our laboratory. The sample was mounted inside an SM4 superconducting split-coil magnet/cryostat (Oxford Instruments), which enabled measurements using magnetic fields of up to 5 T, with sample temperatures down to 1.5 K. The magnetic field and sample temperature were determined with a hall probe (Lakeshore Cryotronics) and a calibrated carbon/glass resistor (Cryogenics Calibrations). Optical absorption spectra were recorded with a Hitachi U-3200 spectrometer.

RESULTS

Direct electrochemical studies

The cyclic voltammetry of *D. africanus* Fd III is shown in Figs. 1 and 2. A single cycle produces an informative picture of the active redox couples present and thus an

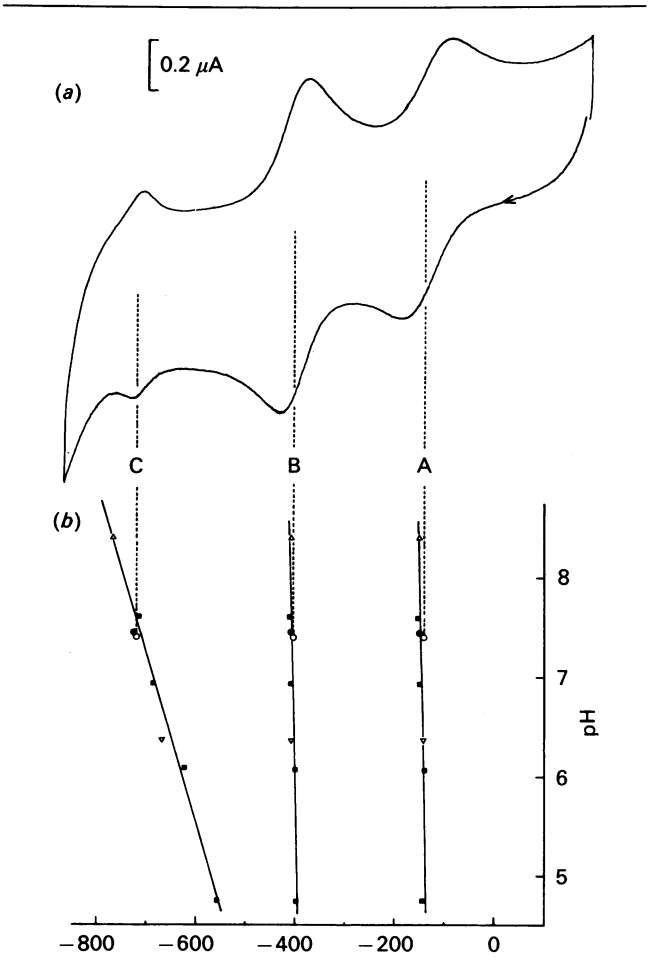

Fig. 1. (a) Cyclic voltammogram of *D. africanus* Fd III and (b) pH-dependence of $E^{0'}$ values

(*a*) Cyclic voltammogram of *D. africanus* Fd III. The protein concentration was 0.11 mM in 20 mM-Hepes buffer, pH 7.40, containing 100 mM-$NaClO_4$, 0.1 mM-EGTA and 1.1 mM-neomycin. The scan rate was 8 $mV \cdot s^{-1}$. The temperature was 2 °C. (*b*) pH-dependence of $E^{0'}$ values. Buffers: ■, 3 mM-Pipes/3 mM-Hepes/3 mM-Taps containing 100 mM-NaCl; △, 20 mM-Taps containing 100 mM-NaCl; ●, 20 mM-Hepes containing 100 mM-NaCl; ○, 20 mM-Hepes containing 100 mM-$NaClO_4$; ▽, 20 mM-Pipes containing 100 mM-NaCl. All solutions contained 0.1 mM-EGTA and 1–2 mM-neomycin. The temperature was 2 °C. Lines show least-squares fits to data points.

immediate guide to the status of clusters throughout the course of chemical or electrochemical manipulations.

Three sets of waves are observed after promotion of electrochemical response at the PGE electrode by addition of 1 mM-neomycin or -tobramycin. To facilitate discussion these have been labelled A, B and C in order of decreasing potential. Although the central positions of waves A and B are essentially independent of pH over the range 5–8, their relative amplitudes are sensitive to various factors. At a freshly polished electrode under conditions of slow scan rate (i.e. $\leqslant 16\ mV \cdot s^{-1}$) the waves are of approximately equal size for samples that have been dialysed against or contain 0.1 mM-EDTA or -EGTA, as shown in Fig. 1. Omission of the treatment with chelators yielded voltammograms in which wave B was enlarged and waves A and C were attenuated. As discussed in the following paper [5], this change arises from ready cluster transformation that is prevented by sequestration of adventitious Fe(II). Details that follow refer to studies made with EGTA-treated solutions. Similar results were obtained regardless of whether the supporting electrolyte was 100 mM-NaCl or -$NaClO_4$.

Waves A are strongly scan-rate-dependent. At 2 °C with a scan rate of $16\ mV \cdot s^{-1}$, $E^{0\prime}$ is -140 ± 10 mV and the peak separation ΔE_p is typically 100 mV. Plots of cathodic peak current (i_{pc}) against (scan rate)$^{\frac{1}{2}}$ are linear up to $16\ mV \cdot s^{-1}$. Thus this electrode process is classically quasi-reversible and diffusion-controlled at low scan rates. As the scan rate is increased (Fig. 2), both cathodic and anodic waves separate (ΔE_p increases), broaden and collapse to expose a new pair of waves A′, with $E^{0\prime} = -140$ mV and $\Delta E_p < 50$ mV at $800\ mV \cdot s^{-1}$. As far as can be estimated from corrections for background, the anodic peak current (i_{pa}) of waves A′ increases proportionately to scan rate over the range 160–$800\ mV \cdot s^{-1}$. Waves A′ are not observed in buffer alone and therefore must be attributed to an adsorbed form of Fd III. It is thus apparent that the electrochemical response of Fd III is a combination of electrode processes involving both adsorbed and freely diffusing molecules [10]. Low scan rates emphasize the latter whereas rapid sweeps detect only the adsorbed couple if diffusion-type electrode kinetics are poor. If, as seems likely, waves A and A′ arise from the same chemical process, then the negligible shift in $E^{0\prime}$ values implies that oxidized and reduced forms correspond to species with similar free energies of adsorption [10].

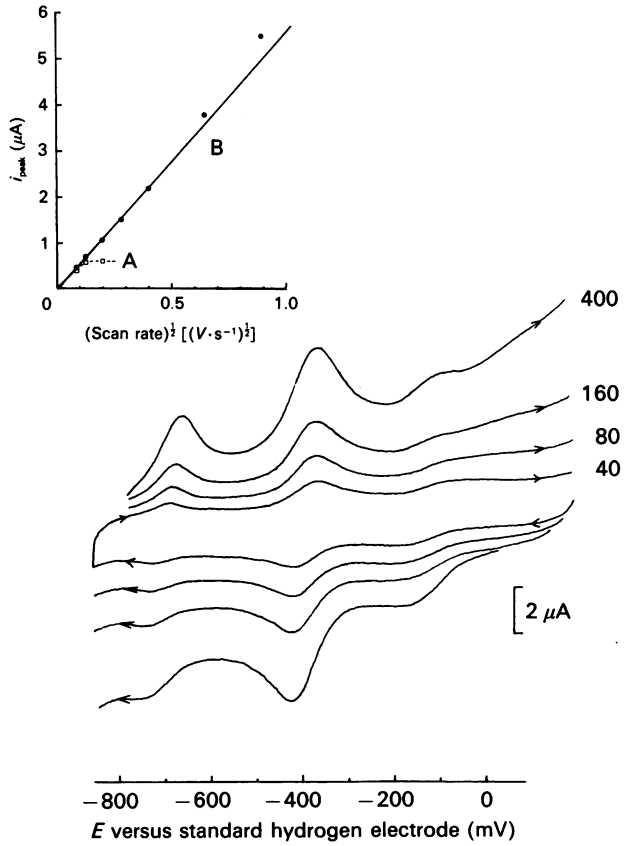

Fig. 2. Scan-rate-dependence of the cyclic voltammetry of *D. africanus* Fd III

The protein concentration was 0.11 mM in solution of 20 mM-Hepes buffer, pH 7.40, containing 100 mM-$NaClO_4$, 0.1 mM-EGTA and 1.1 mM-neomycin. The temperature was 2 °C. Scan rates in $mV \cdot s^{-1}$ are indicated. Inset shows plots of peak currents, for couples A (□, i_{pc}) and B (●, i_{pa}), against (scan rate)$^{\frac{1}{2}}$.

By contrast with the complexity of waves A, waves B correspond to a stable and apparently much faster solution redox couple with $E^{0\prime} = -410 \pm 5$ mV at 2 °C. The peak separation is between 55 and 60 mV over the scan-rate range 4–$800\ mV \cdot s^{-1}$ and plots of anodic peak current against (scan rate)$^{\frac{1}{2}}$ are linear up to $160\ mV \cdot s^{-1}$. Above this a slight upwards deviation is noticeable, which is indicative [10] of an increased relative current contribution from adsorbed protein. Importantly, though, $E^{0\prime}$ does not vary at least up to $800\ mV \cdot s^{-1}$. Neither do the wave shapes alter significantly as a function of either time or scan rate. Thus B corresponds to a redox couple for which heterogeneous electron transfer is effectively diffusion-controlled.

Waves C show a marked pH-dependence. Values of $E^{0\prime}$ vary from −670 mV (pH 6.35) to −726 mV (pH 7.45) to −765 mV (pH 8.40), and amplitudes decrease with increasing pH. However, even at pH 6.35 they are considerably smaller than waves A or B at a scan rate of $16\ mV \cdot s^{-1}$. The pH-dependence broadly suggests $1H^+/1e^-$ stoichiometry. Peak separations are typically 25–30 mV at a scan rate of $8\ mV \cdot s^{-1}$ and increase significantly as this is raised. This suggests that waves C arise from a quasi-reversible adsorbed species. The nature of the species giving rise to waves C is not discussed further in the present paper.

Exhaustive anaerobic electrochemical reduction, typically at −605 mV, of samples containing 0.1–0.2 mM-EDTA or -EGTA gave, for each of seven experiments, charge integrations corresponding to 1.93, 2.06, 1.91, 1.89, 1.90, 1.93 and 1.93 electrons per protein monomer. Partial reduction, in the presence of 1.0 mM-EGTA, to an equilibrium potential of −260 mV consumed 0.91 electron.

In summary therefore the direct voltammetric experiments show the presence of two reducible centres with $E^{0\prime}$ values of $-140\ mV \pm 10$ mV and $-410\ mV \pm 5$ mV at 2 °C. As established by bulk electrolysis, these are present in equimolar amounts, which suggests there is one of each reducible centre per monomeric unit. A further reduction process is observed by cyclic voltammetry, at an $E^{0\prime}$ value of −726 mV (pH 7.45).

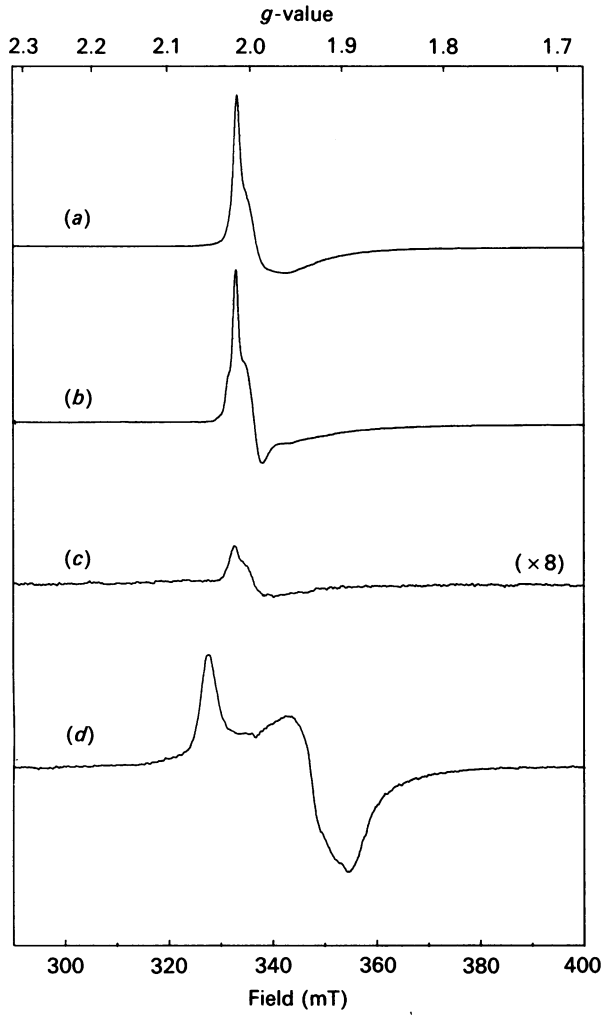

Fig. 3. X-band e.p.r. spectra of *D. africanus* Fd III

Spectra (*a*)–(*d*) were recorded at 11 K with microwave power 2 mW, microwave frequency 9.40 GHz, and modulation amplitude 0.5 mT. No corrections for variations in tube calibration have been made. (*a*) Native (oxidized) Fd. The protein concentration was 526 μM in 0.1 mM-Tris buffer, pH 8.0. Spectrometer gain = 8×10^3. (*b*) Native (oxidized) Fd. The protein concentration was 200 μM in 25 mM-Taps buffer, pH 8.0, containing 50% (v/v) ethanediol. Spectrometer gain = 2.5×10^4. (*c*) Fd electrochemically poised at −260 mV. The protein concentration was 103 μM in 20 mM-Hepes buffer, pH 7.4, containing 100 mM-NaCl, 0.1 mM-EGTA and 1.5 mM-neomycin. Spectrometer gain = 3.5×10^5; number of scans = 2. This spectrum is plotted on an 8-fold magnification. (*d*) Fd electrochemically reduced at −605 mV. The protein concentration was 93 μM in 20 mM-Hepes buffer, pH 7.4, containing 100 mM-NaCl, 0.1 mM-HDTA and 1.25 mM-neomycin. Spectrometer gain = 3.2×10^5; number of scans = 2.

E.p.r. and m.c.d. spectroscopic studies

In order to investigate the chemical nature of couples A and B, we have used direct electrochemical reduction to prepare samples for e.p.r. spectroscopy. During the course of electrolysis of each sample it is possible to assess, rapidly, the extent of reduction and, by measuring a cyclic voltammogram, the molecular integrity of all the redox centres in the ferredoxin.

The X-band e.p.r. spectra from the native, fully oxidized, Fd comprises a slightly anisotropic signal centred on $g = 2.01$ (Figs. 3*a* and 3*b*). The lineshape of this signal is, in general, similar to those observed from proteins containing an oxidized $[3Fe\text{-}4S]^{1+}$ centre [11], namely a low-field sharp positive peak with a shoulder, followed by a much-less-intense broad negative 'tail' to high field. It is, however, sensitive to the buffer composition and the presence of glassing agent (compare, for example, Figs. 3*a* and 3*b*), and additional features can often be observed, in particlar on the low-field edge of the main peak. The temperature-dependence of this signal is similar to that observed for the $[3Fe\text{-}4S]^{1+}$ containing Fd II from *Desulfovibrio gigas* [12]. Assuming a ground state of spin $S = \frac{1}{2}$, double integration of this signal typically yields 0.6–0.7 spin per monomer. For reasons detailed below, we believe that this is an underestimate and that the e.p.r. spectrum in fact represents a single spin.

Direct electrochemical reduction of the Fd to −260 mV, a value approximately midway between $E^{0\prime}$ for couples A and B, consumes a single electron per monomer. It also causes the $g = 2.01$ e.p.r. signal to be almost completely abolished (Fig. 3*c*) and the appearance of a weak broad feature at $g = 12$ (not shown). This signal is similar to that observed in the half-reduced ferredoxin from *Thermus thermophilus* [13], which has been assigned by Hagen and co-workers to the $\Delta M_s = 4$ transition in the $S = 2$ ground state of a reduced [3Fe-4S] cluster. We note that observation of this signal in our samples of *D. africanus* Fd III is complicated by the presence of adventitious Fe(II) ion, which, when co-ordinated to the EDTA, EGTA or HDTA in our buffers, gives low-field spectra.

Two-electron reduction of the Fd, with the cell potential set at −605 mV, generates a further species with an axial e.p.r. spectrum at $g_\perp = 1.93$ and $g_\parallel = 2.05$ (Fig. 3*d*). Double integration of this signal typically yields 1.0 ± 0.1 spin equivalents. Its form and temperature-dependence are consistent with those of a $[4Fe\text{-}4S]^{1+}$ centre. We note that the $g = 12$ signal is also present in this spectrum. The clear implication of these data is that the $g = 2.01$ and $g = 12$ signals are associated with waves A, whereas

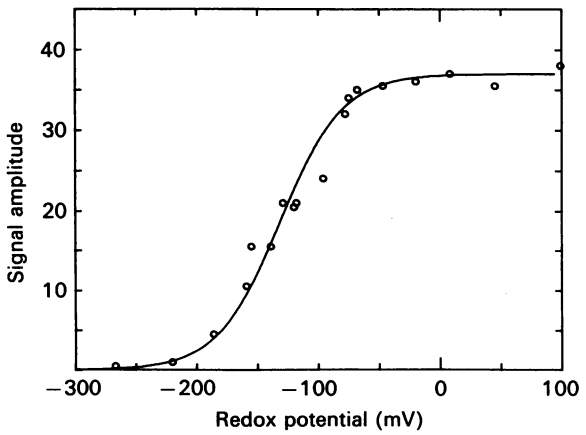

Fig. 4. E.p.r.-monitored redox titration of the $g = 2.01$ signal in *D. africanus* Fd III

Sample conditions were as described in the text.

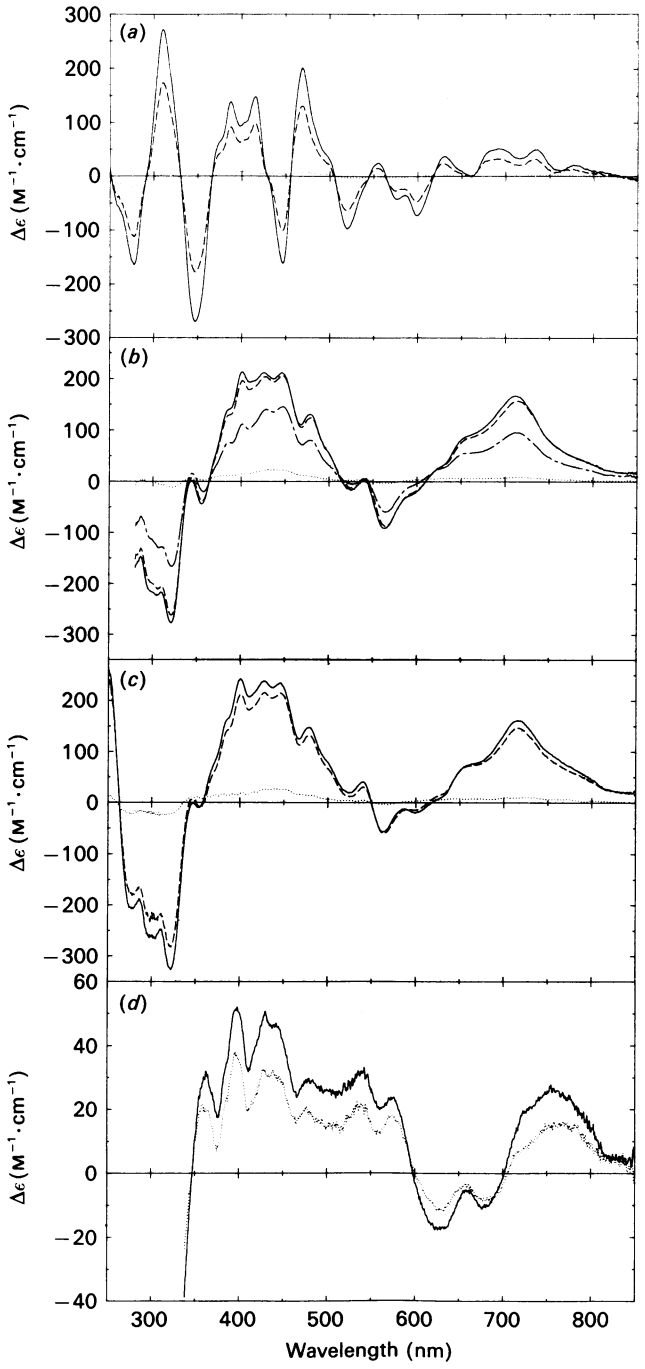

Fig. 5. Low-temperature m.c.d. spectra of *D. africanus* Fd III recorded at 5.00 T and a number of temperatures

(*a*) Native (oxidized) Fd, recorded at 1.6 K (——), 4.2 K (– – –) and 96 K (·····). The protein concentration was 200 μM in 25 mM-Taps buffer, pH 8.0, containing 50% (v/v) ethanediol. The pathlength was 1.17 mm. (*b*) 'One-electron'-reduced Fd, reduced by phenosafranine solution, recorded at 1.6 K (——), 4.2 K (– – –), 10 K (— · —) and 98 K (·····). The protein concentration was 361 μM in 20 mM-Hepes buffer, pH 7.4, containing, 100 mM-NaCl and 50% (v/v) ethanediol. The pathlength was 1.00 mm. (*c*) 'Two-electron'-reduced Fd, reduced by $Na_2S_2O_4$ solution, recorded at 1.6 K (——), 4.22 K (– – –) and 94 K (·····). The protein concentration was 357 μM in 20 mM-Hepes buffer, pH 7.4, containing 100 mM-NaCl and 50% (v/v) ethanediol. The pathlength was 1.00 mm. (*d*) Difference m.c.d. spectrum [(*c*)−(*b*)], showing the additional m.c.d. caused by reduction with the second electron equivalent. A correction for 7% cluster interconversion is included. Temperatures were 1.6 K (——) and 4.2 K (·····).

the $g = 1.93$ spectrum arises from the reduction of the redox centre giving rise to waves B.

To establish this unequivocally we performed potentiometric titrations using dye-mediated electrochemistry at a platinum electrode. These experiments were not carried out in the presence of EDTA or EGTA. The intensity of the $g = 2.01$ signal varies sigmoidally with potential (Fig. 4). Analysis of the profile indicates an electron stoichiometry $n = 1$ with E_m (pH 7.4) = −130 mV. We therefore assign the $g = 2.01$ signal to the oxidized form of couple A. The agreement in redox potential demonstrates the extent to which direct electrochemistry is able to yield for protein redox centres, reduction potentials that are close to bulk equilibrium measurements of E_m. The potentiometric titration using dye-mediated electrochemistry of the $g = 1.94$ signal was, however, less conclusive. Lineshape changes in the e.p.r. spectrum indicative of chemical change confused the analysis and the plot of the resulting signal intensity versus potential displayed substantial error bars (results not shown). The origin of these changes are discussed in the following paper [5].

In order to determine unambiguously the nature of the iron–sulphur sites in *D. africanus* Fd III we have employed low-temperature m.c.d. spectroscopy. Unfortunately, electrochemical preparation of samples for m.c.d. spectroscopy has so far proved problematic. This is because the ethanediol glassing agent necessary for the low-temperature m.c.d. experiment substantially increases the viscosity and hence the reduction half-life. The presence of ethanediol (50%, v/v) in the medium did not significantly shift the $E^{0'}$ values obtained by cyclic voltammetry. Thus samples for m.c.d. were prepared with the use of either $Na_2S_2O_4$ or an appropriate organic redox dye as a reductant. The redox condition of these samples was monitored independently by e.p.r.

The low-temperature m.c.d. spectrum from the native oxidized Fd is given in Fig. 5(*a*). Identical spectra have been obtained from at least four different samples. M.c.d. magnetization curves have been determined for the majority of the bands in the spectrum, at several temperatures between 1.5 K and 10 K. The curves recorded at all wavelengths are superimposable (see, e.g., Fig. 6*a*). The theoretical analysis of m.c.d. magnetizations in terms of the electronic ground-state structure has been discussed elsewhere [14–16]. For an isotropic Kramer's-doublet ground state the *g*-value is simply the inverse of its intercept value (i.e. the intersection of its initial slope and asymptotic limit). The curve in Fig. 6(*a*) therefore indicates a spin $S = \frac{1}{2}$ ground-state doublet with $g = 2.0$. This is consistent with observation of an e.p.r. intercept signal of $g = 2.01$ in this oxidation state.

Fd III reduced by a single electron equivalent was prepared both by a titration with $Na_2S_2O_4$ solution and by using phenosafranine as a reductant. The resulting m.c.d. spectrum (Fig. 5*b*) is temperature- and field-dependent. Magnetization data have been collected from a number of bands, and example curves are given in Figs. 6(*b*)–6(*d*). It is clear that the magnetization characteristic of the spectrum varies substantially with wavelength,

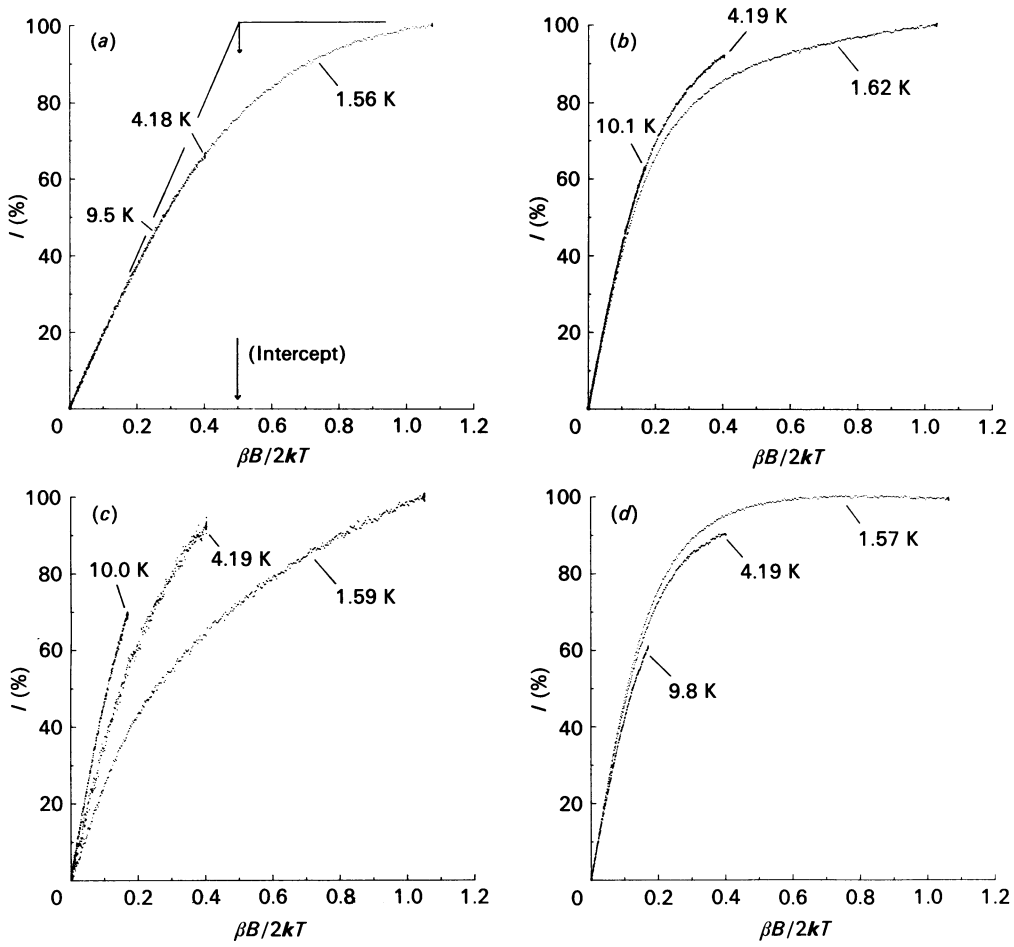

Fig. 6. Low-temperature m.c.d. magnetizations of *D. africanus* Fd III from the spectra in Fig. 5

Magnetizations were recorded with approximate sample temperatures of 1.6 K, 4.2 K and 10 K. Exact temperatures are indicated on each panel. (*a*) Native Fd (Fig. 5*a*) at 327 nm. Indicated on the magnetization curve is the intercept value. (*b*)–(*d*) Half-reduced Fd (Fig. 5*b*) at (*b*) 321.5 nm, (*c*) 564 nm and (*d*) 713 nm.

and that, as a rule, different temperature curves are not co-linear on a $\beta B/2kT$ plot. Theoretical analysis of such curves is a more complex procedure than that outlined above [16]. Preliminary results, however, indicate that they arise from a paramagnet of spin $S = 2$ ground state with a small negative axial zero-field splitting. This is consistent with observation of an e.p.r. signal at $g = 12$ in this oxidation state.

Comparison of these m.c.d. data from native (oxidized) and one-electron-reduced *D. africanus* Fd III with those from other iron–sulphur-cluster-containing proteins is instructive. The peaks, troughs and shoulders in the spectrum from native Fd III, for example, correspond closely to those in the spectrum from the $[3Fe\text{-}4S]^{1+}$-containing Fd II from *D. gigas* [17,18]. In addition, when the spectrum from one-electron-reduced Fd III is compared with those from the reduced [3Fe-4S]-centre-containing proteins such as *D. gigas* Fd II [17,18], inactive aconitase [19] and alkaline Fd I from *Azotobacter chroococcum* [20] and *A. vinelandii* [21] a close similarity between the spectra is seen. This is particularly apparent in the form of the magnetization curves, which vary in a corresponding manner with wavelength. This indicates that the electronic structures of the clusters in these three proteins are similar both in spin and zero-field parameters. In short, the similarity in the m.c.d. and e.p.r. properties of these proteins in two oxidation states requires that they contain a common paramagnetic chromophore. Therefore the low-temperature m.c.d. and e.p.r. data from native and one-electron-reduced Fd III demonstrate conclusively that the voltammetric waves A arise from a $[3Fe\text{-}4S]^{1+,0}$ centre.

Two-electron-reduced ferredoxin, prepared by using a small excess of $Na_2S_2O_4$ solution, gave the m.c.d. spectrum in Fig. 5(*c*). This spectrum is similar in form to that from one-electron-reduced protein, although the intensity has increased, and some changes in form are seen throughout the spectrum. Fig. 5(*d*) shows the difference of the m.c.d. spectra of the two-electron-reduced and one-electron-reduced protein. In calculating this spectrum we have anticipated the results of our subsequent investigations, and corrected for a small percentage of [3Fe-4S] to [4Fe-4S] cluster conversion that always occurred under the conditions necessary for the m.c.d. experiment (see the following paper [5]). This inevitably introduces possible errors into the calculated spectrum. Nevertheless, comparison of this spectrum with those from $[4Fe\text{-}4S]^{1+}$ containing *D. africanus* Fd I and Fd II [8] as well as *Clostridium pasteurianum* Fd [22] shows a general similarity in both form and temperature-

dependence. This is consistent with the presence of the almost axial $g = 1.94$ e.p.r. signal and enables us to assign the species responsible for voltammetric waves B as a $[4Fe\text{-}4S]^{2+,1+}$ cluster.

DISCUSSION

By using a combination of direct electrochemical analysis with studies of low-temperature e.p.r. and m.c.d. spectra we have unambiguously established that, after aerobic extraction from the bacterium *D. africanus*, Fd III contains one [3Fe-4S] and one [4Fe-4S] core. The clusters have $E^{0'}$ values of -140 ± 10 mV and -410 ± 5 mV respectively. The magnetic properties and the m.c.d characteristics of the [3Fe-4S] cluster are very similar to those of the cluster in *D. gigas* Fd II. In the oxidized state the ground state is spin $S = \frac{1}{2}$ with a g-value 2.01, and in the reduced state the cluster is also paramagnetic with spin $S = 2$ that undergoes a small negative axial zero-field splitting ($D \approx -2\ cm^{-1}$). There is no appreciable pH-dependence of the $E^{0'}$ value, in contrast with the situation that occurs in the [3Fe-4S] cluster in *Azotobacter* Fd I [23]. The $[4Fe\text{-}4S]^{n+}$ core cluster cycles between oxidation levels $n = 2$ and 1, being diamagnetic in the former and e.p.r.-active in the latter. Quantitative electrochemical reduction and spin integration of the e.p.r. spectrum due to the $[4Fe\text{-}4S]^{1+}$ centre together establish that there is one [3Fe-4S] and one [4Fe-4S] core per monomeric unit.

The amino acid sequence of Fd III contains only seven cysteine residues separated into two cluster binding domains. This is in contrast with the sequences of the other well-characterized 7Fe Fds such as those from *Thermus* and *Azotobacter*, which contain at least eight cysteine residues (see Fig. 3 in ref. [24]. It is reasonable to assume that the [4Fe-4S] cluster in *D. africanus* Fd III requires four cysteine residues as ligands, since its spectroscopic and redox properties are very similar to the four-iron clusters known to be so co-ordinated in the Fds from *C. pasteurianum* [22], *Bacillus stearothermophilus* and *Bacillus thermoproteolyticus* [25,26]. Thus only three cysteine residues are available to ligate the [3Fe-4S] core. One of the unusual features of the *D. africanus* Fd III amino acid sequence is that it contains an aspartic acid residue at position 14. It is shown in the following paper [5] that it is likely that the carboxylate side chain of this aspartic acid residue can ligand to a [4Fe-4S] core generated by addition of Fe(II) ion to the [3Fe-4S] cluster. We do not consider it likely that the carboxylate group is interacting with the [3Fe-4S] cluster in the 7Fe Fd since the magnetic and m.c.d. properties of this centre are so similar to those of the cluster in *D. gigas* FdII, in which such an interaction is impossible. We therefore propose a distribution of ligands in accordance with the detailed structural analysis proposed by Fukuyama *et al.* [26]. Fig. 7 indicates the assignment.

The X-ray structure of *A. vinelandii* Fd I has recently been redetermined by two groups of workers [1,2]. Although the resolution is quite low it is clear that only three cysteine residues act as ligands to the [3Fe-4S] core and that the [4Fe-4S] core is coordinated by four cysteine residues in a similar pattern to that in Fig. 7. This work on *D. africanus* Fd III confirms that [3Fe-4S] clusters require co-ordination only by three cysteine ligands, one for each iron atom in the core, and that this is so in both the oxidized and the reduced states. It therefore provides evidence against one of the structures discussed by Beinert & Thomson [11] in which four cysteine residues are ligands to the 3Fe cluster and is further evidence for the correctness of the structure proposed on the basis of vibrational spectroscopy for a [3Fe-4S] core bound to only three cysteine ligands [27].

An important element in our analysis is the use of direct electrochemistry between the protein and an electrode surface. Our results show that, when such electrochemistry can be established, cyclic voltammetric analysis provides a rapid and convenient method of monitoring the presence of redox-active centres in the protein. Care must be taken in the interpretation of such data, however, as the scan-rate-dependence of the cyclic voltammetry of *D. africanus* Fd III indicates the contribution by species adsorbed on the electrode surface as well as freely diffusing bulk solution species. It is in the limit of linearity between peak current and $(\text{scan rate})^{\frac{1}{2}}$ that one is observing a process that is dominated by bulk diffusion of free species to and from the electrode, and which the adsorbed species do not significantly contribute. An interesting related observation is the virtual disappearance at higher scan rates of the bulk diffusive voltammetric response of the $[3Fe\text{-}4S]^{1+,0}$ couple while that of the $[4Fe\text{-}4S]^{2+,1+}$ couple is sustained. First, this indicates that care must be used before attempting to gauge active-site stoichiometries, in complex multicentred proteins, from cyclic-voltammetry wave amplitudes alone. Secondly, it is tempting to interpret this behaviour in terms of a lower intrinsic electron-transfer rate for the [3Fe-4S] cluster. Such ideas must also be treated with caution. It may be that the contrasting voltammetries of [4Fe-4S] and [3Fe-4S] clusters may reflect aspects of more fundamental electrochemical significance. For example, in terms of a microscopic model recently proposed for protein electron transfer at PGE electrodes [28], this behaviour demonstrates different microscopic dynamic preconditions, such as binding and orientation, for the oxidation and reduction of two separate centres on a single protein molecule.

Two aspects of our e.p.r. results also deserve comment.

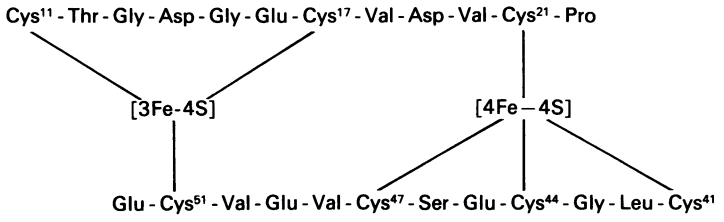

Fig. 7. Proposed assignment of ligands for the [3Fe-4S] and [4Fe-4S] clusters of *D. africanus* Fd III

First, the spectrum from the native Fd is similar to those observed from other [3Fe-4S]$^{1+}$-containing proteins, but depending on buffer composition, additional structure can be observed. In addition, double integration of this signal apparently underestimates the [3Fe-4S]$^{1+}$ cluster concentration as estimated by the m.c.d. and electrochemical analysis. We note that lineshapes of e.p.r. spectra from [3Fe-4S]$^{1+}$ centres have been simulated by using a simple '*g*-strain' model, i.e. assuming a statistical distribution of *g*-values from protein molecules with different conformations [13,29,30]. We, however, currently have no satisfactory explanation for the additional structure or buffer-dependence of the spectra in Figs. 3(*a*) and 3(*b*). The origin of the low-spin integration of this signal is also unclear, although this may be related to difficulties in quantifying the long 'tail' of intensity to high field. Secondly, the e.p.r. spectrum of the reduced [4Fe-4S]$^{1+}$ cluster is not typical of the spectra of the four-iron cluster in reduced 7Fe Fds such as *T. thermophilus* Fd [13] and fully reduced *A. chroococcum* Fd [23]. In these cases the e.p.r. spectrum is a rhombic $S = \frac{1}{2}$ signal containing additional shoulders and peaks commonly assumed to arise from exchange coupling between the reduced [3Fe-4S] cluster ($S = 2$) and the reduced [4Fe-4S] core. In view of the size of Fd III (M_r 6585), which is smaller than that of other 7Fe Fds, it is not clear why such coupling is not evident in the e.p.r. spectrum of the reduced 4Fe cluster. Spectra of the fully reduced state at 3 GHz and 15 GHz were measured early in this investigation (R. Cammack, E. C. Hatchikian & R. Dunham, unpublished work) and indicated that any broadening due to exchange interactions was slight. It was concluded that a large contribution to line broadening was occurring as a result of '*g*-strain'.

In conclusion, this work adds spectroscopic weight to the X-ray crystallographic evidence for the 3Fe cluster in proteins being formulated as $[Fe_3S_4(Cys)_3]^{2-/3-}$ in both accessible oxidation states. Spectroscopic evidence suggests that this is generally true for many 3Fe-cluster-containing proteins. For example, the m.c.d. properties of the reduced states of the 3Fe clusters in a wide variety of proteins are very similar. An interesting exception is the reduced state of the 3Fe cluster in the Fd I from *A. chroococcum* and *A. vinelandii*, which can exist in two states depending upon the solution pH [20,21,23]. Both forms have $S = 2$ and a negative axial zero-field splitting parameter of approx. $-2\ cm^{-1}$. Apart from this, it is likely that there are few (if any) core structure differences of any significance.

This work was supported by grants from the S.E.R.C. to A. J. T., F. A. A. and R. C., from The Royal Society to A. J. T. and to F. A. A., and from P.I.R.S.E.M.–C.N.R.S. to E. C. H.; F. A. A. is a Royal Society University Research Fellow and thanks Dr. H. A. O. Hill (Oxford) for provision of electrochemical facilities. We thank B. Dodemont-Pirlot for assistance with the mediated redox titrations.

REFERENCES

1. Stout, G. H., Turley, S., Sieker, L. C. & Jensen, L. H. (1988) Proc. Natl. Acad. Sci. U.S.A. **85**, 1020–1022
2. Stout, C. D. (1988) J. Biol. Chem. **263**, 9256–9260
3. Adman, E. T., Sieker, L. C. & Jensen, L. H. (1973) J. Biol. Chem. **248**, 3987–3996
4. Bovier-Lapierre, G., Bruschi, M., Bonicel, J. & Hatchikian, E. C. (1987) Biochim. Biophys. Acta **913**, 20–26
5. George, S. J., Armstrong, F. A., Hatchikian, E. C. & Thomson, A. J. (1989) Biochem. J. **264**, 275–284
6. Hatchikian, E. C. & Bruschi, M. (1981) Biochim. Biophys. Acta **634**, 41–51
7. Hatchikian, E. C., Jones, H. E. & Bruschi, N. (1979) Biochim. Biophys. Acta **548**, 471–483
8. Hatchikian, E. C., Cammack, R., Patil, D. S., Robinson, A. E., Richards, A. J. M., George, S. J. & Thomson, A. J. (1984) Biochim. Biophys. Acta **784**, 40–47
9. Armstrong, F. A., Cox, P. A., Hill, H. A. O., Lowe, V. J. & Oliver, B. N. (1987) J. Electroanal. Chem. **217**, 331–366
10. Wopschall, R. H. & Shain, I. (1967) Anal. Chem. **37**, 1514–1527
11. Beinert, H. & Thomson, A. J. (1983) Arch. Biochem. Biophys. **222**, 333–361
12. Gayda, J. P., Bertrand, P., Theodule, F.-X. & Moura, J. J. G. (1982) J. Chem. Phys. **77**, 3387–3391
13. Hagen, W. R., Dunham, W. R., Johnson, M. K. & Fee, J. A. (1985) Biochim. Biophys. Acta **828**, 369–374
14. Thomson, A. J. & Johnson, M. K. (1980) Biochem. J. **191**, 411–420
15. Schatz, P. N., Mowery, R. L. & Krausz, E. R. (1978) Mol. Phys. **35**, 1537–1557
16. Cheesman, M. R. (1988) Ph.D. Thesis, University of East Anglia
17. Thomson, A. J., Robinson, A. E., Johnson, M. K., Moura, J. J. G., Moura, I., Xavier, A. V. & Le Gall, J. (1981) Biochim. Biophys. Acta **670**, 93–100
18. George, S. J. (1986) Ph.D. Thesis, University of East Anglia
19. Johnson, M. K., Thomson, A. J., Richards, A. J. M., Peterson, J., Robinson, A. E., Ramsay, R. R. & Singer, T. P. (1984) J. Biol. Chem. **259**, 2274–2282
20. George, S. J., Richards, A. J. M., Thomson, A. J. & Yates, M. G. (1984) Biochem. J. **224**, 247–251
21. Johnson, M. K., Bennett, D. E., Fee, J. A. & Sweeney, W. V. (1987) Biochim. Biophys. Acta **911**, 81–94
22. Johnson, M. K., Thomson, A. J., Robinson, A. E., Rao, K. K. & Hall, D. O. (1981) Biochim. Biophys. Acta **667**, 433–451
23. Armstrong, F. A., George, S. J., Thomson, A. J. & Yates, M. G. (1988) FEBS Lett. **234**, 107–110
24. Otaka, G. & Ooi, T. (1987) J. Mol. Evol. **26**, 257–267
25. Mullinger, R. N., Cammack, R., Rao, K. K., Hall, D. O., Dickson, D. P. G., Johnson, C. G., Rush, J. D. & Simopoulos, A. (1975) Biochem. J. **151**, 75–83
26. Fukuyama, K., Nagahara, Y., Tsukihara, T., Katsube, Y., Hase, T. & Matsubara, H. (1988) J. Mol. Biol. **199**, 183–193
27. Johnson, M. K., Czernuszewicz, R. S., Spiro, T. G., Fee, J. A. & Sweeney, W. V. (1983) J. Am. Chem. Soc. **105**, 6671–6678
28. Armstrong, F. A., Bond, A. M., Hill, H. A. O., Psalti, I. S. M. & Zoski, C. G. (1989) J. Phys. Chem. **93**, 6485–6493
29. Guigliarelli, B., Gayda, J. P., Bertrand, P. & More, C. (1986) Biochim. Biophys. Acta **871**, 149–155
30. Guigliarelli, B., More, C., Bertrand, P. & Gayda, J. P. (1986) J. Chem. Phys. **85**, 2774–2778

Received 27 April 1989/13 June 1989; accepted 20 June 1989